ISSN : 0974 - 7486 Volume 10 Issue 11

Materials Science

An Indian Journal

Full Paper

MSAIJ, 10(11), 2014 [469-475]

Influence of the Si content in steels on their mechanical and chemical behaviors. Part 2: Properties in corrosion

Elodie Conrath, Patrice Berthod*

Institut Jean Lamour (UMR CNRS 7198), Department CP2S, Faculty of Sciences and Technologies

University of Lorraine, B.P. 70239, 54506 Vandoeuvre-lès-Nancy, (FRANCE)

E-mail : patrice.berthod@univ-lorraine.fr

ABSTRACT

The four ternary steels Fe-xSi-0.01C (x=1 to 2.5%) elaborated in the first part of this work to study the effect of the silicon content and the plastic deformation on hardness, and on high temperature oxidation at this can be encountered during hot-rolling, were considered to study the effects of the same parameters on the corrosion rate in acidic aqueous solution. The additional experiments done to complete the preceding ones for characterizing the various solicitations to which iron sheets can be exposed at the different steps of their manufacturing were cyclic polarization runs performed in a 2N sulphuric solution. A lot of parameters characterizing these curves were analyzed with regards to the Si content and to the plastically deformed state. The greatest influence on the results is due to the presence of 1% and more of silicon. This element lowers the corrosion rate in the active state and modifies the shapes of both the potential-increasing part and the potential-decreasing part of the cyclic polarization curves by comparison with pure polycrystalline iron. The better resistance against active corrosion is an additional beneficial effect of silicon which improved hardness and compression resistance at room temperature as well as high temperature oxidation behaviour, as previously seen in the first part of this work.

KEYWORDS

Ferritic steel;
Silicon content;
Plastic deformation;
Corrosion;
Electrochemical measurements.

INTRODUCTION

The effect of a forged state – or more generally of plastic strains – on the surface reactivity of metallic materials has been under great interest for several decades. Surface reactivity can be with gases at high temperatures or with liquid solutions. In a first part[1] of this work four alloys Fe-xSi-0.01C (wt.%), with x=1, 2, 2.2 and 2.5 were first studied in short oxidation at high temperature without or with preliminary deformation in compression. But it can be interesting to also study their behaviour in corrosion by acidic solutions at room temperature to better know what can occur for such alloys in such industrial environments.

Studies concerning the possible changes in aqueous corrosion behaviour resulting from plastic deformation were driven several tens of years ago. Some of them were for example realized in the cases of steels with different compositions/microstructures (e.g. ferritic, austenitic…) or metallurgical states (martensitic…) in

various aqueous media, for instance aerated water or acid sulphuric acidic solutions[1-4]. The influence of hardening, which was generally observed for such metallic materials, was an acceleration of corrosion in the active state. In contrast the effect on the corrosion behaviour of non-ferrous alloys was more variable[5-7], but it was often observed that plastic deformation favours also faster corrosion. Many metallic pieces are, in service, in contact with corrosive aqueous solutions (the most often acidic), and at the same time highly stressed and consequently plastically deformed, simultaneously or not. They are thus affected by stress corrosion in the periods when they are still to subjected to mechanical stresses, and at other times to classical corrosion when no stress is applied. In the last case it is of importance to know the rate with which hardened/ plastically deformed pieces are corroded.

In this second part of a this work the not-compressed (as-cast) and compression-plastically deformed Fe-xSi-0.01C alloys, more shortly named Fe-xSi alloys, were studied in corrosion in an acidic solution similar to the ones with which some industrial laminated steels may be in contact just after their cooling. This was done notably by considering, in addition to the effect of the plastic deformation, the possible influence of the silicon content.

EXPERIMENTAL

Elaboration, sample preparation, compression rates

One can shortly remind that the chemical compositions were initially defined to work on simplified steels which are however still close to the industrial ones manufactured as coils (extra low carbon, possible presence in small quantities of other elements added for targeting specific mechanical properties, as silicon). In this work four ternary alloys, all on the Fe-0.01C-xSi–type, were elaborated by foundry with the following wished compositions: Fe-1Si-0.01C, Fe-2Si-0.01C, Fe-2.2Si-0.01C and Fe-2.5Si-0.01C (in weight percents). The 40g–ingots, obtained from pure elements: Fe (Alfa Aesar, purity > 99.97%), Si (Alfa Aesar, 99.999%) and graphite, resulted from fusion and solidification occurred in the water-cooled copper crucible of a high frequency induction furnace (CELES). These high temperature synthesis operations were performed under 300 millibars of pure Argon (<3ppm O_2). The ingots were cut in order to obtain samples for some of them compression runs, for all (as-cast or compressed) high temperature oxidation tests or not, and finally for all (compressed or not, oxidized or not) metallography observations and microstructure characterization[1].

For the present study not-compressed (as-cast) parts of the four ingots were taken to prepare electrodes, as well as parts of the compressed samples (obtained deformation rates: -33.63% for the "Fe-1Si" alloy, -24.28% for the "Fe-2.0Si" alloy, -29.09% for the "Fe-2.2Si" alloy and -22.55% for the "Fe-2.5Si" alloy).

Electrode preparation and electrochemical runs

For preparing each electrode, the resin part of the metallographic sample was drilled until reaching the other side of the metallic parts. A not-covered end of a partly plastic-covered copper wire was introduced, put in contact with the other side of the steel sample, and fixed by introducing and compressing copper ribbon in the hole. The emerging steel surface which will be characterized in corrosion, initially resulting from the cutting of the compressed sample, was parallel to the axis of compression deformation earlier done.

The electrochemical experiments performed to characterize the corrosion behaviours of these samples in acidic solution were run at room temperature in a H_2SO_4 2N solution. This was done by using a three-electrodes cell (the studied sample as working electrode, a graphite rod as auxiliary electrode and a Saturated Calomel Electrode (SCE) as potential reference electrode) and a potensiostat model 263A of Princeton Applied Research driven by the M352 software from EG&G/Princeton.

The experiments which were done were cyclic polarizations. They consisted of a potential-increasing part between E_{ocp} – 250mV up to 1.9V at +5mV/s, followed by a potential-decreasing part between 1.9V down to E_{ocp} – 250mV at -5mV/s. The potential-increasing parts of the later files were also considered to perform Tafel calculations in order to specify potential and current of corrosion, as well as the anodic and cathodic Tafel coefficients.

RESULTS AND DISCUSSION

Analysis of the effect of hardening on the obtained cyclic polarization curves

The example of a whole cyclic polarization curve is displayed in Figure 0 (here: the one corresponding to the not-compressed "Fe-1%Si" alloy). The potential-increasing part (E-increasing part named "E^" in this graph) starts at low potential with rather high values of the logarithm of the absolute value of the current density (cathodic, then negative). About 250mV higher, the applied potential reaches the corrosion potential ($E_{corr^}$, shown by "e0"). Thereafter the logarithm of the absolute value of the current density (now positive) increases again, until reaching a passivation critical intensity (I_{cp1}, shown by "i1"). Just after the current density falls down to a first low value (a kind of first passivation plateau, I_{pass1} shown by "i3") at a kind of first passivation potential (E_{pass1}, shown by "e2"). A little after and for higher potential, a new decrease in current density occurs, down to a second passivation current density (I_{pass2}, shown by "i5") at an apparent second passivation potential (E_{pass2}, shown by "e4"). The anodic current density remains then rather constant until transpassivation occurs (corresponding potential $E_{transpass}$ and maximal intensity $I_{transpass}$ shown by "e7" and "i6" respectively). The oxidation of water the solution itself (the "solvent's wall") starts just after, at a potential E_{solvox} shown by "e8").

The potential-decreasing part (E-decreasing part named "Ev" in this graph) starts at the end of the E-increasing part. With the decrease in applied potential from the very high value earlier reached, the anodic current density decreases until reaching an inclined plateau which probably includes the transpassivation lump. An average value of the passivation current density (I_{pass3}, shown by "Ia") may be noted. The passivation state is lost later at a lost-passivation potential ($E_{lostpass}$, shown by ""Eb") and the current density jumps to very high values before stabilizing at a constant value $I_{plateau}$ (shown by "Id") when the applied potential reaches a plateau potential ($E_{plateau}$, shown by "Ec"). During the potential decrease from the last value the current density stays constant and starts to decrease when the applied potential approaches the new corrosion potential $E_{corr\ v}$ (shown by "Ee").

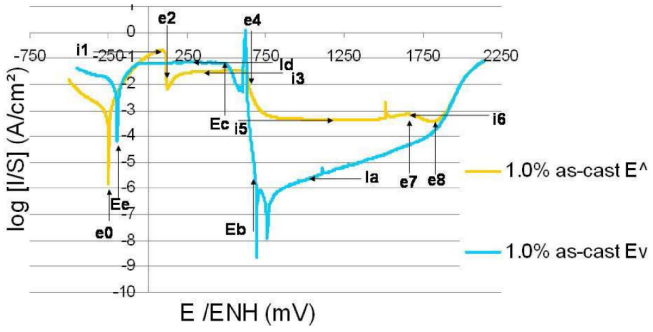

Figure 0 : Example illustrating the obtained cyclic polarization curves (E- increasing part in orange and E-decreasing part in blue on the same graph)

Most of the cyclic polarization curves look like the one previously described. The E-increasing parts of the curves obtained for the as-cast state and the compressed state are presented together in Figure 1 (for the Fe-1Si and Fe-2.0Si alloys) and in Figure 2 (for the Fe-2.2Si and Fe-2.5Si alloys). One can see that all these curves correspond to the general description done above. For the three first alloys (from 1 to 2.2%Si) there are no significant differences between the E-increasing curves obtained in the as-cast state and the ones obtained in the compressed states. One can maybe note that the first passivation plateau seems to be reached

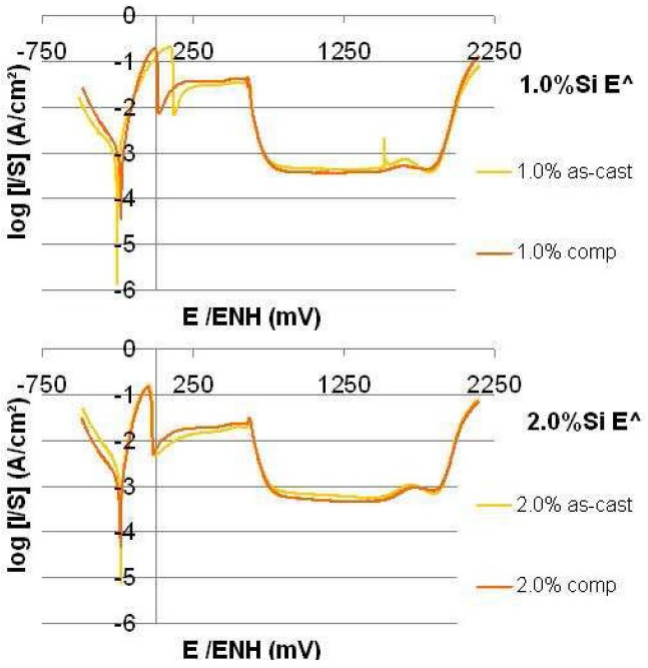

Figure 1 : Potential-increasing parts of the cyclic polarization curves obtained for the as-cast state (clear orange) and the compressed state (dark orange) of the Fe-1Si (top) and Fe-2Si (bottom) alloys

sooner (i.e. at a lower value of the applied potential) for the compressed state than for the as-cast one (seen for 1%Si and 2.2%Si). Differences are much more visible for the 2.5%Si-containing alloy for which the E-increasing curve obtained for the compressed state presents very high values of current density, whatever the applied potential.

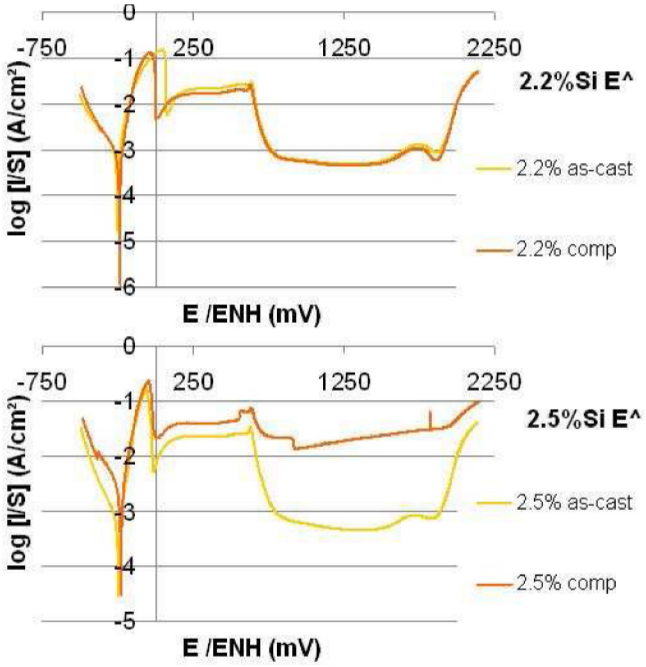

Figure 2 : Potential-increasing parts of the cyclic polarization curves obtained for the as-cast state (clear orange) and the compressed state (dark orange) of the Fe-2.2Si (top) and Fe-2.5Si (bottom) alloys

The values of the different parameters listed in the previous paragraph are given in TABLE 1 for the E-increasing parts. Studying these values confirm that there is not systematic and significant differences between the curves in their different E-increasing parts, except when some of the values obtain ed for the compressed Fe-2.5Si alloy are compared to the analogous ones of the other {alloy; state} combinations.

What was said about the influence of the hardening on the E-increasing parts of the cyclic polarization curves can be repeated about the E-decreasing parts (Figure 3 and Figure 4): no strong effect. However the compressed 2.5%Si alloy seems showing a specific behaviour, characterized by particularly high values of current densities. This is true again for the values of the

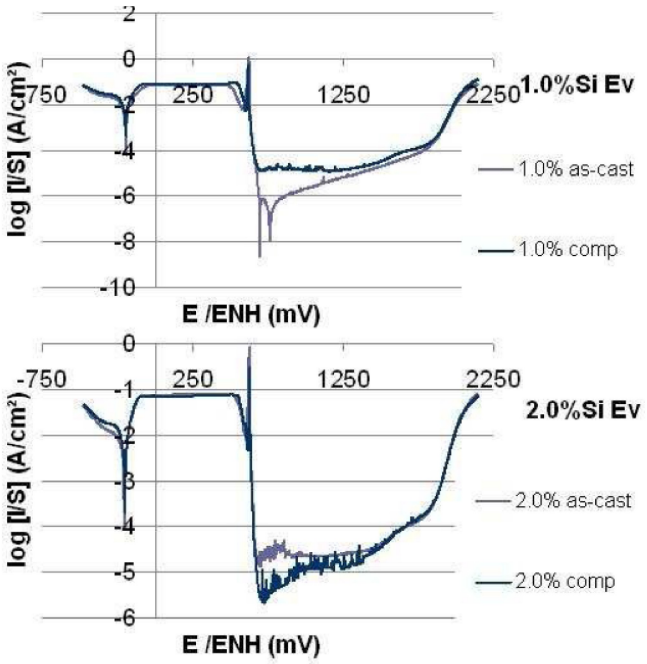

Figure 3 : Potential-decreasing parts of the cyclic polarization curves obtained for the as-cast state (clear blue) and the compressed state (dark blue) of the Fe-1Si (top) and Fe-2Si (bottom) alloys

TABLE 1 : Characteristic values of potential and current density noted on the potential-increasing parts of the cyclic polarization curves

Alloy (wt.%Si)	State	E_{corr} ↑ (e0)	I_{cp1} (i1)	E_{pass1} (e2)	I_{pass1} (i3)	E_{pass2} (e4)	I_{pass2} (i5)	$I_{transpass}$ (i6)	$E_{transpass}$ (e7)	E_{solvax} (e8)
		V/SCE	mA/cm²	V/SCE	mA/cm²	V/SCE	µA/cm²		V/SCE	
Fe-1Si	As-cast	-0.492	199	-0.126	29.7	+0.402	443	675	1.37	1.58
	Compressed	-0.466	191	-0.224	35.9	+0.382	373	521	1.40	1.56
Fe-2.0Si	As-cast	-0.469	154	-0.261	15.6	+0.397	621	1059	1.45	1.61
	Compressed	-0.472	141	-0.268	18.7	+0.398	466	922	1.47	1.61
Fe-2.2Si	As-cast	-0.496	144	-0.174	21.8	+0.408	487	1294	1.51	1.63
	Compressed	-0.478	130	-0.246	16.8	+0.412	458	1084	1.51	1.64
Fe-2.5Si	As-cast	-0.484	160	-0.272	22.8	+0.402	497	854	1.48	1.58
	Compressed	-0.469	232	-0.289	39.1	+0.411	21160	/	/	/

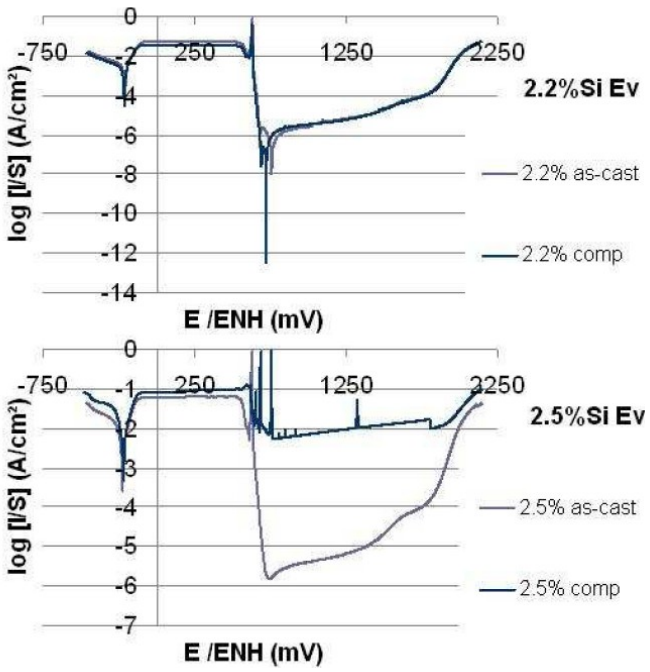

Figure 4 : Potential-decreasing parts of the cyclic polarization curves obtained for the as-cast state (clear blue) and the compressed state (dark blue) of the Fe-2.2Si (top) and Fe-2.5Si (bottom) alloys

different parameters given in TABLE 2 for the E-decreasing parts of the curves.

Analysis of the effect of the silicon content on the obtained cyclic polarization curves

The same E-increasing parts and E-decreasing parts of the cyclic polarization curves are respectively plotted in Figure 5 and Figure 6 (E-increasing parts in the as-cast and compressed states), and in Figure 7 and Figure 8 (E-decreasing parts in the as-cast and compressed states) to allow better comparison between the alloys themselves for revealing possible effects of the silicon contents. Obviously there are no differences between the curves, except for the ones corresponding to the Fe-2.5%Si in the compressed state.

Tafel analysis of the potential-increasing parts of the curves

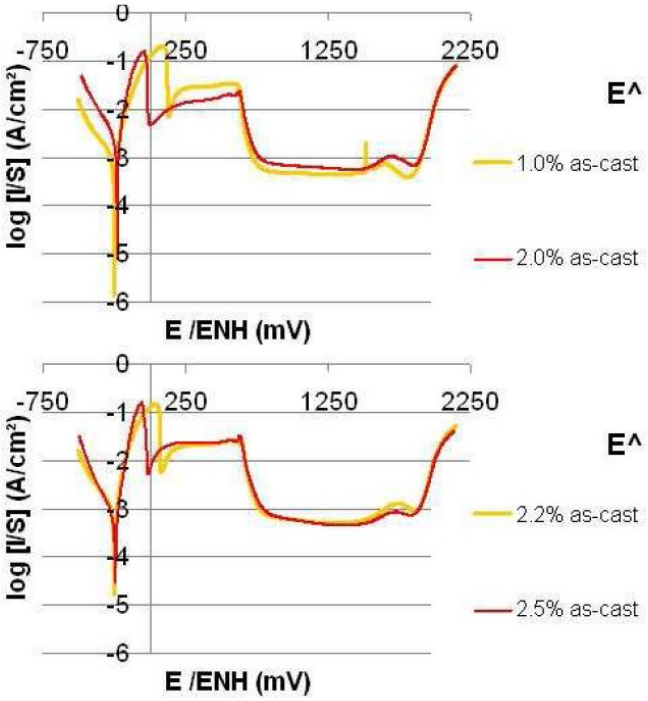

Figure 5 : Influence of the silicon content on the potential-increasing parts of the cyclic polarization curves obtained for the as-cast state (top : Fe-1Si (clear orange) and Fe-2Si (dark orange); bottom : Fe-2.2Si (clear orange) and Fe-2.5Si (dark orange))

The [E(I=0) – 250mV, E(I=0) + 250mV] part of the E-increasing parts of each curve was analyzed using the Tafel method. This led to the values of Tafel anodic and cathodic coefficients and of corrosion po-

TABLE 2 : Characteristic values of potential and current density noted on the potential-decreasing parts of the cyclic polarization curves

Alloy (wt.%Si)	State	I_{pass3} (Ia)	$E_{lostpass}$ (Eb)	$E_{plateau}$ (Ec)	$I_{plateau}$ (Id)	E_{corr} ↓ (Ec)
		µA/cm²	V/SCE	V/SCE	mA/cm²	V/SCE
Fe-1Si	As-cast	1.71	+0.450	+0.248	64.5	-0.436
	Compressed	12.5	+0.422	+0.300	79.1	-0.438
Fe-2.0Si	As-cast	27.8	+0.415	+0.261	76.3	-0.445
	Compressed	12.9	+0.412	+0.306	69.3	-0.442
Fe-2.2Si	As-cast	3.66	+0.420	+0.268	49.4	-0.450
	Compressed	2.40	+0.480	+0.276	32.0	-0.454
Fe-2.5Si	As-cast	4.66	+0.456	+0.280	61.5	-0.466
	Compressed	9095	+0.445	+0.363	111	-0.459

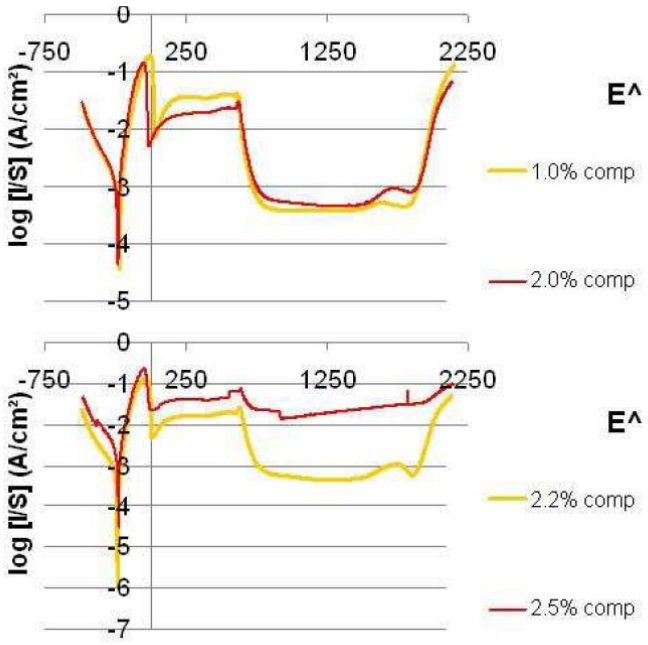

Figure 6 : Influence of the silicon content on the potential-increasing parts of the cyclic polarization curves obtained for the compressed state (top : Fe-1Si (clear orange) and Fe-2Si (dark orange); bottom : Fe-2.2Si (clear orange) and Fe-2.5Si (dark orange))

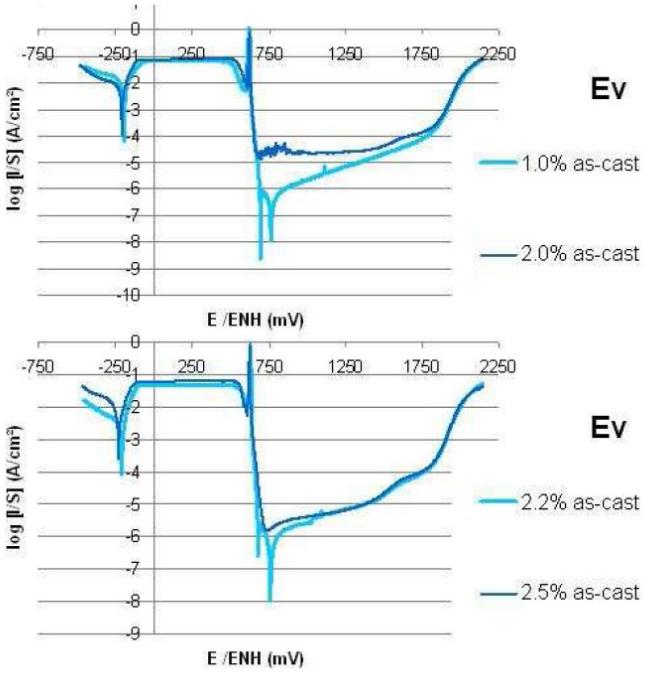

Figure 7 : Influence of the silicon content on the potential-decreasing parts of the cyclic polarization curves obtained for the as-cast state (top : Fe-1Si (clear orange) and Fe-2Si (dark orange); bottom : Fe-2.2Si (clear orange) and Fe-2.5Si (dark orange))

tential and current density given in TABLE 3. The Tafel anodic coefficients are all close to the theoretic value of

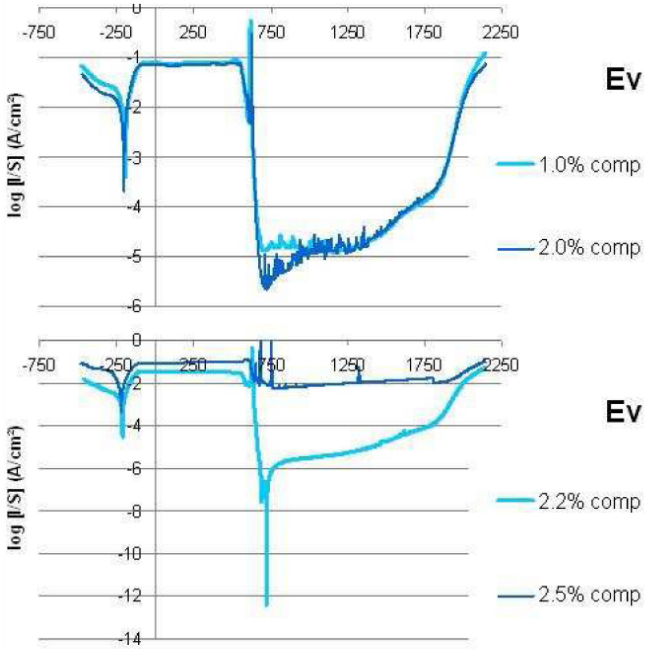

Figure 8 : Influence of the silicon content on the potential-decreasing parts of the cyclic polarization curves obtained for the compressed state (top : Fe-1Si (clear orange) and Fe-2Si (dark orange); bottom : Fe-2.2Si (clear orange) and Fe-2.5Si (dark orange))

about 60mV / decade corresponding to a reaction M $\rightarrow M^{2+}$ + 2 electrons at room temperature while the Tafel cathodic coefficients are a little too high to well correspond to the H^+ + 1 electron $\rightarrow$ ½ H_2 reaction. The corrosion potentials are not really the same for all the curves and there is no systematic influence neither of the hardened state nor of the silicon content. The same comments can be done about the corrosion current density.

General commentaries

There is thus globally no real or systematic influence of the plastic deformation and of the silicon content on the cyclic polarization curves obtained for these four Si-containing alloys. The case of the compressed Fe-2.5Si needs to be verified before really comparing it to the other, because of its very curious behaviour. When the results obtained in this work are compared with previous ones, for example obtained in similar conditions of elaboration and compression test, one can remark that the shape of the curves, common to almost all the alloys studied in the present work, is rather special: passivation in two times during the E-increasing part, existence of a plateau in the E-decreasing part…

TABLE 3 : Tafel coefficients, corrosion potential and corrosion current densities issued from the Tafel method applied to the E-increasing part of the cycling polarization curves centred on E(I=0)±250mV

Alloy (wt.%Si)	State	β_a	β_c	E_{corr}	I_{corr}
		mV / decade		mV / ECS	mA / cm²
Fe-1Si	As-cast	75.56	262.3	-492.0	1.111
	Compressed	69.77	232.3	-466.7	1.151
Fe-2.0Si	As-cast	69.88	190.9	-469.1	2.170
	Compressed	67.04	246.4	-472.6	1.445
Fe-2.2Si	As-cast	77.06	351.5	-490.4	1.270
	Compressed	61.20	221.7	-478.0	0.787
Fe-2.5Si	As-cast	62.06	188.3	-483.1	0.690
	Compressed	74.03	230.2	-468.6	2.651

This is very different with what is usually found for pure iron in the same conditions of electrolyte and of experiment (parameters values of cyclic polarization), and also for a carbon steel elaborated following the same route[9] (only one anodic peak…). It is possible that the presence of silicon in the present alloys is responsible of this curious phenomena which maybe results of two successive passivations, an earlier first one due to the oxidation of silicon (with a limited protective effect due to the two low concentrations in Si in all alloys), and a more usual second one due to the formation of a layer of oxi-hydroxide of iron covering the surface. The values of I_{corr} (around 1mA/cm²) significantly lower than the ones obtained for the carbon steel earlier studied[9] (around 4 mA/cm²) were probably obtained here thanks to the presence of Si in the present alloys.

CONCLUSIONS

It was found in the first part of this work that the presence of Si improved the hardness and the mechanical resistance of these alloys against compression deformation as well as it slowed the oxidation rate at 750°C for the first ten minutes of stage. Another beneficial effect of this element was found in this second part: the lowering of the corrosion rate in the active state. Other effects were also found elsewhere in the cyclic polarization curves, such as the double passivation plateau, phenomenon which was partly interpreted but which needs further investigations. In contrast, the effect of compression seems to be much more limited than for other alloys, at least on the cyclic polarization curves. This may be to be perhaps also attributed to the presence of silicon which acts in corrosion without being concerned by plastic deformation as it is the case for the iron polycrystal in which Si is present only in solid solution.

REFERENCES

[1] E.Conrath, P.Berthod, L.Aranda; Materials Science: An Indian Journal, in press.

[2] A.Ben Bachir, H.Triche; Mémoire Scientifique Revue de Métallurgie, **71**, 9 (**1974**).

[3] M.Saled, L.Aries, H.Triche; Mémoire Scientifique Revue de Métallurgie, **71**, 621 (**1974**).

[4] M.S.Khoma; Fiziko-Khimicheskaya Mekhanika Materialov, **30**, 125 (**1994**).

[5] X.C.Li, R.L.Eadie, J.L.Luo; Corrosion Engineering Science and Technology, **43**, 297 (**2008**).

[6] P.Berthod; Materials Science: An Indian Journal, **5**, 161 (**2009**).

[7] E.Akiyama, Z.Zhang, Y.Watanabe, K.Tsuzaki; Journal of Solid State Electrochemistry, **13**, 277 **(2009)**.

[8] W.Y.Guo, J.Sun, J.S.Wu; Materials Characterization, **60**, 173 **(2009)**.

[9] E.Conrath, P.Berthod; Materials Science: An Indian Journal, **9**, 131 (**2013**).